Published in final edited form as:
FEBS J. 2008 January ; 275(1): 59–68. doi:10.1111/j.1742-4658.2007.06171.x.

Structure–function analysis of the filamentous actin binding domain of the neuronal scaffolding protein spinophilin

Herwig Schüler[1,*] and **Wolfgang Peti**[2]

[1]Max Delbrück Center for Molecular Medicine, Berlin-Buch, Germany

[2]Department of Molecular Pharmacology, Physiology, and Biotechnology, Brown University, Providence, RI, USA

Abstract

Spinophilin, a neuronal scaffolding protein, is essential for synaptic transmission, and functions to target protein phosphatase-1 to distinct subcellular locations in dendritic spines. It is vital for the regulation of dendritic spine formation and motility, and functions by regulating glutamatergic receptors and binding to filamentous actin. To investigate its role in regulating actin cytoskeletal structure, we initiated structural studies of the actin binding domain of spinophilin. We demonstrate that the spinophilin actin binding domain is intrinsically unstructured, and that, with increasing C-terminal length, the domain shows augmented secondary structure content. Further characterization confirmed the previously known crosslinking activity and uncovered a novel filamentous actin pointed-end capping activity. Both of these functions seem to be fully contained within residues 1–154 of spinophilin.

Keywords

F-actin; intrinsically unstructured protein; pointed-end capping protein; spinal plasticity; spinophilin

Dendritic spines, globular protrusions from neuronal dendrites in the central nervous system, are the major sites of excitatory signal transduction in dendrites. During the past few years, it has been realized that dendritic spines are highly dynamic structures, both during development and in the adult nervous system. Dendritic spine morphology changes rapidly and can be visualized on a minutes time scale (e.g. [1,2]).

Dendritic plasticity is believed to be central for normal brain functioning [3]. The turnover of dendritic spines is directly involved in memory formation [4], and changes in spine plasticity caused by epileptic seizures may underlie cognitive deficits in epilepsy patients [5]. Thus, a comprehensive description of the molecular components involved in the regulation and maintenance of dendritic spine morphology is fundamental to our understanding of the functions of the central nervous system.

Correspondence H. Schüler, Max Delbrück Center for Molecular Medicine, 13125 Berlin-Buch, Germany Fax: 0049-6221-564643 Tel: 0049-6221-568284 herwig.schueler@med.uniheidelberg.de. W. Peti, Department of Molecular Pharmacology, Physiology, and Biotechnology, Brown University, Box G-E3, Providence, RI 02912, USA Fax: 001-401-8636087 Tel: 001-401-8636084 wolfgang_peti@brown.edu.

[*]**Present address** Department of Parasitology, Heidelberg University Medical School, Germany

The molecular details that underlie the regulation of spine morphology have advanced considerably in recent years. As actin is the only cytoskeletal component present in spines, actin interacting proteins are prime candidates for the regulation of dendritic spine plasticity [6]. Indeed, spine motility is powered by the polymerization of actin [7,8]. In addition, actin regulators, such as profilin [1,9] and rho-dependent pathways (e.g. [10,11]), have already been shown to influence spine morphology.

Spinophilin (Genbank ID PPP1R9B: protein phosphatase-1 regulatory subunit 9B), also known as neurabin-II, is a neuronal scaffolding protein involved in the regulation of dendritic spine morphology [12,13] (reviewed in [14]). Spinophilin binds and bundles actin polymers, thereby stabilizing actin structures in the spines [15,16]. Moreover, spinophilin can recruit rho-family GTPases, influencing actin reorganization [17]. Spinophilin also targets protein phosphatases (protein phosphatase-1, PP1) [13,18,19] and binds to glutamatergic receptors [20–22]. It is currently believed that spinophilin functions to target PP1 to glutamate [α-amino-3-hydroxy-5-methyl-4-isoxazolpropionate (AMPA) and *N*-methyl-D-aspartate (NMDA)] receptors, and thereby modulates their activity and trafficking through regulation of their phosphorylation state [23]. Secondly, spinophilin targets PP1 to the post-synaptic densities by providing a link to the microfilament system [24].

Spinophilin shares its general domain structure and about 65% overall sequence identity with its neuronal isoform neurabin (Fig. 1A). Spinophilin, although ubiquitously expressed, is predominantly found in neurones, whereas neurabin is expressed almost exclusively in neuronal cells, generally at lower levels than spinophilin. Despite their similarity, they do not compensate for one another [23,25,26]. Both spinophilin and neurabin contain N-terminal filamentous actin (F-actin) binding, PP1 binding, PDZ and C-terminal coiled-coil domains. In addition, neurabin, but not spinophilin, contains a sterile α motif (SAM) domain [27] in its C-terminus, whereas spinophilin, but not neurabin, may possess a dopamine receptor / α-adrenergic interacting domain in its N-terminus, possibly between spinophilin residues 200 and 400 [20]. The structures of the spinophilin and neurabin PDZ [22] and neurabin SAM [27] domains have been solved recently by NMR spectroscopy.

Spinophilin interaction with F-actin is regulated by phosphorylation of its actin binding domain (ABD) by protein kinase-A (PKA) [28], calcium / calmodulin-dependent kinase II [29], cyclin-dependent kinase-5 and extracellular signal-regulated kinase-2 (ERK2) [30]. PKA phosphorylates three serine residues located in the N-terminal region of spinophilin, namely Ser94, Ser177 and, to some extent, Ser100, whereas ERK2 phosphorylates Ser15 and Ser205. Phosphorylation of spinophilin ABD leads to an attenuated interaction with F-actin. Phosphorylation of these serine residues may be reversed by different phosphatases, thus restoring the F-actin binding capacity of spinophilin [30,31], but the pathway constituents that regulate actin binding through phosphate signalling are unknown.

We have undertaken a systematic and detailed structural and functional analysis of the ABD of spinophilin. We show that residues 1–154 of spinophilin are both necessary and sufficient to mediate F-actin binding. Critically, we also show that residues 1–154 of spinophilin and longer spinophilin ABD constructs (residues 1–221 and 1–305 of spinophilin) are intrinsically unstructured, as tested by NMR and CD spectroscopy. In addition, we show that, at low molar ratios, spinophilin ABDs bind and crosslink actin polymers. However, at high molar ratios, they cap F-actin polymers. Thus, we provide evidence for an F-actin capping activity of spinophilin.

Results and Discussion

Spinophilin construct design and production

Spinophilin has previously been shown to bind to actin polymers via its N-terminal domain [16]. Furthermore, the spinophilin–F-actin interaction has been partially characterized *in vitro* and *in vivo*. Here, we set out to study spinophilin ABD and its interaction with F-actin using an array of biophysical characterization tools to gain insights into the mechanism of the interaction. Proteins comprising spinophilin ABD residues 1–154, 1–221, 1–305, 154–221, 154–301 and 221–305 were produced in *Escherichia coli* and purified to homogeneity, free of affinity tags used for increased solubility during expression and purification. Thus, untagged spinophilin constructs were analysed in this study, eliminating possible interaction of actin with the hexahistidine tags on spinophilin.

Spinophilin and neurabin ABDs are predicted to be unstructured

We used secondary structure prediction and disorder recognition software to analyse the sequence of spinophilin ABD (residues 1–305). Initial analysis showed that the sequence of spinophilin was highly biased towards disorder-inducing amino acids (i.e. proline and charged amino acids [32]), suggesting that it is unstructured. Six different prediction programs were then used to estimate the secondary structure content of N-terminal fragments of human and rat spinophilin and human neurabin. The results showed that only approximately 20% of the spinophilin ABD sequence was predicted to adopt a classified secondary structure (Table 1), with the remainder predicted to be in random coil. In a subsequent step, the programs IUPRED, VSL2 and PONDR were used to detect regions of disorder in the ABDs of spinophilin and neurabin. As shown in Fig. 1, these programs also predicted a high degree of disorder in the ABDs of spinophilin and neurabin. On the basis of these analyses, spinophilin and neurabin ABDs were predicted to be intrinsically unstructured proteins (IUPs).

Spinophilin ABD is intrinsically unstructured

NMR spectroscopy is the only atomic resolution technique able to resolve the structural and dynamic characteristics of IUPs. Therefore, to experimentally verify the *in silico* predictions, we carried out one-dimensional ^{1}H NMR experiments (Fig. 2A,B). The NMR spectra of these constructs perfectly resembled the spectra of unfolded proteins: they showed no signs of either amide proton dispersion, which is indicative of hydrogen bonding in secondary structure elements, or ring current shifted methyl groups, which are caused by the interaction of methyl groups with aromatic side chains in the hydrophobic core of folded proteins. This suggests that these recombinant spinophilin protein constructs are intrinsically unstructured. To further verify this result, we recorded far-UV CD spectropolarimetric spectra of the spinophilin ABD constructs (Fig. 2C), which enables rapid analysis of the overall secondary structure content of proteins. The CD spectra of residues 1–154, 1–221 and 1–305 of spinophilin were indicative of random coil structures, with a negative absorption around 202 nm. However, the CD spectra for all three protein domain constructs showed a negative absorption around 222 nm, indicating differentially increasing amounts of α-helical content. Using $[\theta]_{222\ nm}$, the α-helical content was calculated to be 12%, 22% and 30% for residues 1–154, 1–221 and 1–305 of spinophilin, respectively (details in Experimental procedures). Thus, both NMR and CD spectroscopy showed experimentally that all spinophilin ABDs were intrinsically unstructured. However, these unstructured proteins, similar to their folded counterparts, displayed different properties. The core F-ABD, the first approximately 160 residues, seemed to be mostly unstructured, behaving like a random coil polymer. Additional C-terminal residues in the longer fragments (residues 1–221 and 1–305 of spinophilin) showed more secondary structure, as revealed by CD spectroscopy. The percentage amino acid composition was uniform within these three

constructs, with one exception: the number of valine residues was doubled in the 1–221 and 1–305 sequences of spinophilin. Thus, the increasingly structured C-terminal regions of residues 1–221 and 1–305 of spinophilin were rich in hydrophobic valine residues. This augmented hydrophobic density could form the hydrophobic nucleus for increased tertiary interactions and secondary structure formation, probably explaining the experimental differences in the CD spectra. Finally, this was supported by empirical observations, which indicated that residues 1–154 of spinophilin degraded more rapidly (24–36 h) than residues 1–221 and 1–305 (~ 5–6 days), when stored at 4 °C, indicating an easier access for proteases to the putative random coil structure of residues 1–154 of spinophilin.

Thus, our experimental NMR and CD data clearly demonstrated that the spinophilin ABD constructs were largely disordered, and that their secondary structure content increased with their C-terminal length.

Despite being intrinsically unstructured, spinophilin ABD is active

It was critical to verify that spinophilin ABDs were biologically active. This was accomplished using F-actin cosedimentation assays. The spinophilin proteins were incubated with calf brain γ-actin under polymerizing conditions and subjected to ultracentrifugation. Residues 1–154, 1–221 and 1–305 of spinophilin sedimented with actin polymers when added at substoichiometric amounts (4 : 1 F-actin : spinophilin construct molar ratio; Fig. 3A). Therefore, this experiment showed specific binding activity towards F-actin of our recombinant spinophilin domains, in spite of their intrinsically unstructured nature. By contrast, additional spinophilin constructs, comprising additional fragments of spinophilin's ABD (residues 154–221, 221–305 and 154–305 of spinophilin), did not cosediment with F-actin filaments (Fig. 3A). Together, these data show that residues 1–154 of spinophilin are sufficient to mediate the spinophilin interaction with F-actin. Furthermore, fragments lacking residues 1–154 of spinophilin cannot interact with actin polymers. This contrasts with a previous study [33], where a second actin binding site was identified in residues 154–305 of spinophilin.

To further verify that our recombinant rat spinophilin ABD constructs functioned identically to wild-type spinophilin, we studied their activity under transient covalent modifications. Phosphorylation at Ser94 and / or Ser177, mediated by cAMP-dependent PKA, has been shown to suppress the actin binding activity of spinophilin from rat [28,29] (Ser177 is not conserved in human and mouse; however, PKA phosphorylation of mouse spinophilin Ser94 is sufficient to suppress its association with F-actin [34]). As illustrated in Fig. 3B, residues 1–221 of spinophilin, treated with PKA, showed a substantially reduced capacity to cosediment with actin polymers. This shows that our recombinant spinophilin, like wild-type spinophilin, is responsive to kinase regulation.

Spinophilin F-ABD is capable of F-actin reorganization

Spinophilin has been shown to crosslink actin polymers *in vitro* [16]. To study the effects of spinophilin ABD on the overall morphology of F-actin, we used fluorescence microscopy of rhodamine–phalloidin-labelled actin polymers (Fig. 4). As expected, actin polymers alone appeared as elongated fluorescent filaments (Fig. 4, top panel). The addition of residues 1–154, 1–221 or 1–305 of spinophilin (4 : 1 F-actin : spinophilin molar ratio) strongly induced the crosslinking of actin polymers. The resulting filament network resembled that obtained with other crosslinking proteins, such as fascin [35,36], filamin [37] and cortexillin [38]. In the presence of these ABD constructs, the concentrations of fluorescent actin polymers appeared to be higher because of the precipitation of crosslinked actin polymer networks onto the glass surface. In agreement with our cosedimentation results, residues 154–221 and 154–305 of spinophilin did not influence the overall morphology of F-actin (Fig. 4).

These results show that the crosslinking of actin polymers *in vitro* does not require any additional regions outside the core ABD residues 1–154 of spinophilin. Furthermore, although the dimerization of spinophilin is achieved via its C-terminal coiled-coil domain (Fig. 1A), our results demonstrated that residues 1–154 of spinophilin are able to bind to several actin polymers at a time. At least two potential scenarios can explain these results. First, residues 1–154 of spinophilin may have the ability to form dimers, which would result in two F-actin binding sites, one in each dimer. As size exclusion chromatography indicated that this sequence (residues 1–154) of spinophilin is monomeric in solution, this would implicate F-actin binding as an activating step for dimer formation. Second, an alternative explanation is the existence of two F-actin binding sites, separated by a flexible linker, within residues 1–154 of spinophilin. As an IUP with little recognizable secondary structure, as demonstrated by CD spectroscopy, this sequence (residues 1–154) of spinophilin shows dramatically increased flexibility when compared with natively folded proteins. This increased flexibility would enable the existence of two F-actin binding sites and a putative flexible linker with much fewer residues when compared with folded proteins.

The observed F-actin crosslinking activity was clearly more pronounced with the longer spinophilin ABD constructs, especially residues 1–305 of spinophilin, a difference which was not resolved in the sedimentation assay (Fig. 3). This may indicate that the region 154–305 modulates the relative angle of the two putative actin binding sites. On the basis of published data, this may also be caused by different effective concentrations of the spinophilin constructs, as this has been shown to shift the activity of other proteins between F-actin bundling and crosslinking [39].

Spinophilin is a pointed-end capping protein

In the cosedimentation assays, we noticed that residues 1–221 of spinophilin, when added in equimolar amounts, cosedimented with F-actin, but also induced a shift of actin from the pellet (F-actin) to the supernatant (G-actin; Fig. 3C) fraction. This cosedimentation activity was also detected for residues 1–154 and 1–305 of spinophilin, but not with residues 154–221, 154–305 and 221–305 of spinophilin (not shown). A shift of F-actin from the pellet to the supernatant fraction may be explained by either sequestration of actin monomers or fragmentation (by capping and possibly severing) into polymer stubs that will not sediment under our experimental conditions. The addition of the spinophilin ABD constructs at equimolar ratios (1 : 1) resulted in the appearance of short actin polymer stubs (shown for residues 1–305 of spinophilin in Fig. 4), as visualized by fluorescence microscopy, consistent with a shift to the nonsedimentable fraction described above for the pelleting assays. As expected, the same results were obtained with all three spinophilin constructs that bound actin, but not with those that did not bind actin. Notably, residues 1–154 of spinophilin also induced a significant appearance of short actin polymers (not shown).

We quantified this effect by measuring the length distribution of actin polymers alone and in the presence of equimolar spinophilin constructs (see histograms in Fig. 4). Actin-only controls displayed a mean filament length of 4.28 μm, which is in excellent agreement with the values reported in the literature [40,41]. The mean filament length decreased to 2.94 μm in the presence of an equimolar amount of residues 1–305 of spinophilin, an effect which is apparent from Fig. 4. This effect cannot be explained by mass action of an actin polymer bundling or crosslinking protein at higher concentrations. Rather, we propose that these observations indicate a polymer capping activity by spinophilin ABD. This concept is supported by the well-documented effect of actin capping proteins on actin polymer networks; for example, the addition of villin to a filamin-crosslinked actin network resulted in solvation of the gel and the appearance of short, fragmented polymers [42]. Moreover, further information can be derived from the length distributions of actin polymers. As demonstrated and discussed in detail by Kuhlman [41], Gaussian distributions of polymer

length are expected initially for actin polymers with both ends free to exchange subunits with the solution. By contrast, pointed-end capping accelerates the turnover exchange kinetics, such that a steady-state exponential polymer length distribution is obtained. Consistent with this, we observed a Gaussian distribution of polymer length for actin alone. However, when an equimolar amount of residues 1–305 of spinophilin was added, we detected a change to an exponential distribution, which is indicative of pointed-end capping (histograms in Fig. 4). These results strongly indicate that spinophilin ABD functions as an F-actin capping protein.

In summary, we propose that spinophilin ABD has two different actin binding properties: polymer crosslinking and lower affinity pointed-end polymer capping and possibly severing.

Experimental procedures

Molecular cloning, protein expression and purification

Three different spinophilin ABD constructs (residues 1–154, 1–221 and 1–305) have been reported to express in bacterial expression systems as hexahistidine (His6) or glutathione *S*-transferase (GST) fusion proteins. We used *Rattus norvegicus* cDNA (DBSOURCE AF016252.1) to generate six spinophilin ABD constructs: residues 1–154, 1–221, 1–305, 154–221, 154–305 and 221–305. These were subcloned in parallel into different expression vectors in order to optimize recombinant production procedures [43]. The highest soluble expression yields were identified for maltose binding protein (MBP) and GST expression tagged constructs. The positively expressing constructs were grown on a large scale by inoculating a 100 mL culture of BL21(DE3)RIL cells (Stratagene, La Jolla, CA, USA) in Luria–Bertani medium containing kanamycin (50 $\mu g \cdot mL^{-1}$) and chloramphenicol (34 $\mu g \cdot mL^{-1}$), and grown overnight at 37 °C with shaking at 250 r.p.m. The next morning, the cells were diluted 1 : 50 in Luria–Bertani medium with appropriate antibiotics and grown at 37 °C with shaking at 250 r.p.m. to an absorbance at 600 nm (A_{600}) of 0.5–0.6. The cultures were placed at 4 °C and the shaker temperature was adjusted to 18 °C. Expression of the spinophilin ABD constructs was induced using 1 mM isopropyl thio-β-D-galactoside. The cell cultures were grown for approximately 18 h at 18 °C, harvested by centrifugation, and the cell pellets were stored at −80 °C until purification.

For purification, N-terminal His6-GST or His6-MBP tags were used. The pellets were resuspended in His-tag specific lysis buffer (50 mM Tris pH 8, 5 mM imidazole, 500 mM NaCl, 0.1% Triton-X, protease inhibitors; Complete EDTA-free, Roche, Indianapolis, IN, USA). The cells were lysed by three passes through a C3 Emulsiflex cell cracker (Avestin, Ottawa, ON, Canada) and cell debris was removed by centrifugation (40 000 ***g***/30 min/4 °C). The clarified lysates were filtered through a 0.22 μm membrane (Millipore, Billerica, MA, USA) and loaded onto HisTrap HP columns (GE Healthcare, Piscataway, NJ, USA) equilibrated with 50 mM Tris pH 8.0, 5 mM imidazole and 500 mM NaCl. The proteins were eluted with a gradient of 5–100% 50 mM Tris pH 8, 500 mM imidazole, 500 mM NaCl over 36 column volumes and collected in 1-mL fractions. Eluted proteins were analysed by SDS-PAGE and the fractions containing pure target protein were pooled. Complete cleavage of the purification tag was achieved using tobacco etch virus NIa protease overnight at 4 °C under steady rocking. Spinophilin constructs were then dialysed against 50 mM Tris pH 7.5, 250 mM NaCl for 5 h, and further purified by a second immobilized metal-ion affinity chromatography step (removal of MBP/GST and tobacco etch virus protease). At this stage, proteins were typically 90–95% pure, as judged by SDS-PAGE analysis. Finally, the samples were concentrated and size exclusion chromatography was performed (Superdex 75 26/60; 20 mM sodium phosphate pH 6.5; 50 mM NaCl; GE Healthcare). Spinophilin protein concentrations were determined using the BCA Protein Assay Kit (Pierce, Rockford, IL, USA) and stored as aliquots at −80 °C. On thawing, the proteins were subjected to

ultracentrifugation at 200 000 ***g*** for 15 min in a Beckman Maxima (Beckman-Coulter, Fullerton, CA, USA), kept on ice, and used the same day.

Nonmuscle γ-actin was purified from bovine brain [44,45]. Briefly, the method involved affinity purification of profilin–actin complexes on poly-L-proline sepharose, enrichment of actin by a cycle of polymerization and depolymerization, isoactin separation by hydroxyapatite chromatography, and a final gel filtration step.

Phosphorylation of spinophilin constructs

Spinophilin constructs (200 pmol) were incubated with the catalytic subunit of PKA (New England Biolabs, Ipswich, MA, USA) overnight, according to the manufacturer's protocol.

Secondary structure prediction

For protein secondary structure prediction, six methods with high success rates (http://cubic.bioc.columbia.edu/eva/) were selected: APSSP2 [46], NORS [47], PORTER [48], PROF [49], PSIPRED [50] and SPRITZ [51]. To estimate protein disorder, we used the programs IUPRED [52], VSL2 [53] and CHARGE-HYDROPATHY ANALYSIS [54] employing the PONDR® server (http://www.pondr.com).

NMR spectroscopy

NMR measurements were performed at 298 K on a Bruker AvanceII 500 MHz spectrometer (Bruker Bio-Spin, Billerica, MA, USA) using a TCI HCN-z cryoprobe; 10% D_2O was added to the samples.

CD polarimetry

CD spectra of protein solutions of residues 1–154 (4.3 μM), 1–221 (3.3 μM) and 1–305 (3.8 μM) of spinophilin in 20 mM sodium phosphate buffer pH 6.5, 50 mM NaCl were recorded using a Jasco J-815 spectropolarimeter (JASCO, Easton, MD, USA) and 2 mm cuvettes. CD spectra were recorded in identical buffer solutions and a background subtraction was performed. The means of three scans are reported. All spectra were recorded at 25 °C. Molar ellipticity was calculated using the mean residue weights for each protein. The helical content was estimated from the molar ellipticity at 222 nm using: % α-helix = $(-[\theta]_{222\ nm} + 3000)/39\ 000)$ [55].

Cosedimentation assay

Samples of actin (5 μM) were induced to polymerize by the addition of 1 mM $MgCl_2$ + 0.15 M KCl in the presence of different concentrations of the spinophilin constructs, and incubated at room temperature for 2–3 h. Samples were subjected to ultracentrifugation at 200 000 ***g*** for 45 min at 22 °C in a Beckman Maxima (Beckman-Coulter). Equal amounts of the supernatants and pellets were analysed by SDS-PAGE and Coomassie staining.

Fluorescence microscopy

Actin polymers (5 μM) formed under the above conditions were supplemented with 100 nM rhodamine–phalloidin (Invitrogen/Molecular Probes, Carlsbad, CA, USA) and incubated for 15 min at room temperature on coverslips in the presence of spinophilin constructs at different molar ratios. Samples were mounted in Vectashield (Vector Laboratories, Burlingame, CA, USA) and imaged using a × 100 Fluoroplan oil immersion lens on a Zeiss Axiovert M200 microscope (Carl Zeiss, Göttingen, Germany), and images were captured using a CoolSnap HQ camera (Photometrics, Tucson, AZ, USA) and METAMORPH imaging software (Molecular Devices, Downingtown, PA, USA). Actin polymer length measurements were carried out using SCION IMAGE software (Scion Corporation, Frederick, MD, USA). Polymers were sorted into 1 μm bins, their length distributions were plotted, and their

mean filament length was determined by either Gaussian or exponential fits [41]. Polymers shorter than 1 μm were omitted from the analysis [41]. Because of their extensive overlap, we did not attempt to measure the length of crosslinked actin polymers.

Acknowledgments

The authors would like to thank R. Page for careful reading of the manuscript. WP would like to thank J. Hudak, C. Park, T. Ju and J.-M. Palermino for help with the experiments. HS would like to thank E. E. Wanker for providing laboratory space and equipment. CD measurements were performed in the RI-INBRE Research Core Facility and in the NSF/EPSCoR Proteomics Core Facility (supported by NSF 0554548). The project described was supported by Grant Number R01NS056128 from the National Institute of Neurological Disorders and Stroke to WP. The content is solely the responsibility of the authors and does not necessarily represent the official views of the National Institute of Neurological Disorders and Stroke or the National Institutes of Health. WP is the Manning Assistant Professor for Medical Science at Brown University. HS is a fellow of the Deutsche Forschungsgemeinschaft (DFG). This work was supported by an EMBO Short Term Fellowship to HS.

Abbreviations

ABD	actin binding domain
ERK2	extracellular signal-regulated kinase-2
F-actin	filamentous actin
GST	glutathione *S*-transferase
IUP	intrinsically unstructured protein
MBP	maltose binding protein
PKA	protein kinase-A
PP1	protein phosphatase-1
PPP1R9B	protein phosphatase-1 regulatory subunit 9B
SAM	sterile α motif

References

1. Ackermann M, Matus A. Activity-induced targeting of profilin and stabilization of dendritic spine morphology. Nat Neurosci 2003;6:1194–1200. [PubMed: 14555951]
2. Matus A. Actin-based plasticity in dendritic spines. Science 2000;290:754–758. [PubMed: 11052932]
3. Harms KJ, Dunaevsky A. Dendritic spine plasticity: looking beyond development. Brain Res 2006;4 doi:10.1016/j.brainres.2006.02.094.
4. Lamprecht R, LeDoux J. Structural plasticity and memory. Nat Rev Neurosci 2004;5:45–54. [PubMed: 14708003]
5. Wong M. Modulation of dendritic spines in epilepsy: cellular mechanisms and functional implications. Epilepsy Behav 2005;7:569–577. [PubMed: 16246628]
6. Schubert V, Dotti CG. Transmitting on actin: synaptic control of dendritic architecture. J Cell Sci 2007;120:205–212. [PubMed: 17215449]
7. Fischer M, Kaech S, Knutti D, Matus A. Rapid actin-based plasticity in dendritic spines. Neuron 1998;20:847–854. [PubMed: 9620690]
8. Dunaevsky A, Tashiro A, Majewska A, Mason C, Yuste R. Developmental regulation of spine motility in the mammalian central nervous system. Proc Natl Acad Sci USA 1999;96:13438–13443. [PubMed: 10557339]
9. Schubert V, Da Silva JS, Dotti CG. Localized recruitment and activation of RhoA underlies dendritic spine morphology in a glutamate receptor-dependent manner. J Cell Biol 2006;172:453–467. [PubMed: 16449195]

10. Pilpel Y, Segal M. Activation of PKC induces rapid morphological plasticity in dendrites of hippocampal neurons via Rac and Rho-dependent mechanisms. Eur J Neurosci 2004;19:3151–3164. [PubMed: 15217371]
11. Tashiro A, Yuste R. Regulation of dendritic spine motility and stability by Rac1 and Rho kinase: evidence for two forms of spine motility. Mol Cell Neurosci 2004;26:429–440. [PubMed: 15234347]
12. Nakanishi H, Obaishi H, Satoh A, Wada M, Mandai K, Satoh K, Nishioka H, Matsuura Y, Mizoguchi A, Takai Y. Neurabin: a novel neural tissue-specific actin filament-binding protein involved in neurite formation. J Cell Biol 1997;139:951–961. [PubMed: 9362513]
13. Allen PB, Ouimet CC, Greengard P. Spinophilin, a novel protein phosphatase 1 binding protein localized to dendritic spines. Proc Natl Acad Sci USA 1997;94:9956–9961. [PubMed: 9275233]
14. Sarrouilhe D, di Tommaso A, Metaye T, Ladeveze V. Spinophilin: from partners to functions. Biochimie 2006;88:1099–1113. [PubMed: 16737766]
15. Burnett PE, Blackshaw S, Lai MM, Qureshi IA, Burnett AF, Sabatini DM, Snyder SH. Neurabin is a synaptic protein linking p70 S6 kinase and the neuronal cytoskeleton. Proc Natl Acad Sci USA 1998;95:8351–8536. [PubMed: 9653190]
16. Satoh A, Nakanishi H, Obaishi H, Wada M, Takahashi K, Satoh K, Hirao K, Nishioka H, Hata Y, Mizoguchi A, et al. Neurabin-II/spinophilin. An actin filament-binding protein with one pdz domain localized at cadherin-based cell–cell adhesion sites. J Biol Chem 1998;273:3470–3475. [PubMed: 9452470]
17. Ryan XP, Alldritt J, Svenningsson P, Allen PB, Wu GY, Nairn AC, Greengard P. The Rho-specific GEF Lfc interacts with neurabin and spinophilin to regulate dendritic spine morphology. Neuron 2005;47:85–100. [PubMed: 15996550]
18. Hsieh-Wilson LC, Allen PB, Watanabe T, Nairn AC, Greengard P. Characterization of the neuronal targeting protein spinophilin and its interactions with protein phosphatase-1. Biochemistry 1999;38:4365–4373. [PubMed: 10194355]
19. Terry-Lorenzo RT, Carmody LC, Voltz JW, Connor JH, Li S, Smith FD, Milgram SL, Colbran RJ, Shenolikar S. The neuronal actin-binding proteins, neurabin I and neurabin II, recruit specific isoforms of protein phosphatase-1 catalytic subunits. J Biol Chem 2002;277:27716–27724. [PubMed: 12016225]
20. Smith FD, Oxford GS, Milgram SL. Association of the D2 dopamine receptor third cytoplasmic loop with spinophilin, a protein phosphatase-1-interacting protein. J Biol Chem 1999;274:19894–19900. [PubMed: 10391935]
21. Yan Z, Hsieh-Wilson L, Feng J, Tomizawa K, Allen PB, Fienberg AA, Nairn AC, Greengard P. Protein phosphatase 1 modulation of neostriatal AMPA channels: regulation by DARPP-32 and spinophilin. Nat Neurosci 1999;2:13–17. [PubMed: 10195174]
22. Kelker MS, Dancheck B, Ju T, Kessler RP, Hudak J, Nairn AC, Peti W. Structural basis for spinophilin–neurabin receptor interaction. Biochemistry 2007;46:2333–2344. [PubMed: 17279777]
23. Feng J, Yan Z, Ferreira A, Tomizawa K, Liauw JA, Zhuo M, Allen PB, Ouimet CC, Greengard P. Spinophilin regulates the formation and function of dendritic spines. Proc Natl Acad Sci USA 2000;97:9287–9292. [PubMed: 10922077]
24. Hu XY, Huang H, Roadcap DW, Shenolikar SS, Xia H. Actin-associated neurabin–protein phosphatase-1 complex regulates hippocampal plasticity. J Neurochem 2005;95:1841–1851.
25. Allen PB, Zachariou V, Svenningsson P, Lepore AC, Centonze D, Costa C, Rossi S, Bender G, Chen G, Feng J, et al. Distinct roles for spinophilin and neurabin in dopamine-mediated plasticity. Neuroscience 2006;140:897–911. [PubMed: 16600521]
26. Stafstrom-Davis CA, Ouimet CC, Feng J, Allen PB, Greengard P, Houpt TA. Impaired conditioned taste aversion learning in spinophilin knockout mice. Learn Mem 2001;8:272–278. [PubMed: 11584074]
27. Ju T, Ragusa MJ, Hudak J, Nairn AC, Peti W. Structural characterization of the neurabin sterile alpha motif domain. Proteins 2007;69:192–198. [PubMed: 17600833]

28. Hsieh-Wilson LC, Benfenati F, Snyder GL, Allen PB, Nairn AC, Greengard P. Phosphorylation of spinophilin modulates its interaction with actin filaments. J Biol Chem 2003;278:1186–1189. [PubMed: 12417592]
29. Grossman SD, Futter M, Snyder GL, Allen PB, Nairn AC, Greengard P, Hsieh-Wilson LC. Spinophilin is phosphorylated by Ca^{2+} /calmodulin-dependent protein kinase II resulting in regulation of its binding to F-actin. J Neurochem 2004;90:317–324. [PubMed: 15228588]
30. Futter M, Uematsu K, Bullock SA, Kim Y, Hemmings HC Jr, Nishi A, Greengard P, Nairn AC. Phosphorylation of spinophilin by ERK and cyclin-dependent PK 5 (Cdk5). Proc Natl Acad Sci USA 2005;102:3489–3494. [PubMed: 15728359]
31. Terry-Lorenzo RT, Roadcap DW, Otsuka T, Blanpied TA, Zamorano PL, Garner CC, Shenolikar S, Ehlers MD. Neurabin/protein phosphatase-1 complex regulates dendritic spine morphogenesis and maturation. Mol Biol Cell 2005;16:2349–2362. [PubMed: 15743906]
32. Dyson HJ, Wright PE. Intrinsically unstructured proteins and their functions. Nat Rev Mol Cell Biol 2005;6:197–208. [PubMed: 15738986]
33. Barnes AP, Smith FD III, VanDongen HM, VanDongen AM, Milgram SL. The identification of a second actin-binding region in spinophilin/neurabin II. Brain Res Mol Brain Res 2004;124:105–113. [PubMed: 15135218]
34. Uematsu K, Futter M, Hsieh-Wilson LC, Higashi H, Maeda H, Nairn AC, Greengard P, Nishi A. Regulation of spinophilin Ser94 phosphorylation in neostriatal neurons involves both DARPP-32-dependent and independent pathways. J Neurochem 2005;95:1642–1652. [PubMed: 16300646]
35. Tseng Y, Fedorov E, McCaffery JM, Almo SC, Wirtz D. Micromechanics and ultrastructure of actin filament networks crosslinked by human fascin: a comparison with α-actinin. J Mol Biol 2001;310:351–366. [PubMed: 11428894]
36. Ishikawa R, Yamashiro S, Kohama K, Matsumura F. Regulation of actin binding and actin bundling activities of fascin by caldesmon coupled with tropomyosin. J Biol Chem 1998;273:26991–26997. [PubMed: 9756949]
37. Cortese JD, Frieden C. Effect of filamin and controlled linear shear on the microheterogeneity of F-actin/gelsolin gels. Cell Motil Cytoskeleton 1990;17:236–249. [PubMed: 2176572]
38. Stock A, Steinmetz MO, Janmey PA, Aebi U, Gerisch G, Kammerer RA, Weber I, Faix J. Domain analysis of cortexillin I: actin-bundling, PIP_2-binding and the rescue of cytokinesis. EMBO J 1999;18:5274–5284. [PubMed: 10508161]
39. Tseng Y, Schafer BW, Almo SC, Wirtz D. Functional synergy of actin filament cross-linking proteins. J Biol Chem 2002;277:25609–25616. [PubMed: 12006593]
40. Burlacu S, Janmey PA, Borejdo J. Distribution of actin filament lengths measured by fluorescence microscopy. Am J Physiol 1992;262:C569–C577. [PubMed: 1312777]
41. Kuhlman PA. Dynamic changes in the length distribution of actin filaments during polymerization can be modulated by barbed end capping proteins. Cell Motil Cytoskeleton 2005;61:1–8. [PubMed: 15776462]
42. Nunally MH, Powell LD, Craig SW. Reconstitution and regulation of actin gel–sol transformations with purified filamin and villin. J Biol Chem 1981;256:2083–2086. [PubMed: 6893985]
43. Peti W, Page R. Strategies to maximize heterologous protein expression in Escherichia coli with minimal cost. Protein Expr Purif 2007;51:1–10. [PubMed: 16904906]
44. Lindberg U, Schutt CE, Hellsten E, Tjader AC, Hult T. The use of poly(L-proline)-Sepharose in the isolation of profilin and profilactin complexes. Biochim Biophys Acta 1988;967:391–400. [PubMed: 3196757]
45. Schuler, H.; Karlsson, R.; Lindberg, U. Purification of non-muscle actin. In: Celis, J., editor. Cell Biology: A Laboratory Handbook. Academic Press; New York: 2005. p. 165-172.
46. Kaur H, Raghava GP. Prediction of beta-turns in proteins from multiple alignment using neural network. Protein Sci 2003;12:627–634. [PubMed: 12592033]
47. Rost B, Yachdav G, Liu J. The PredictProtein server. Nucleic Acids Res 2004;32:W321–W326. [PubMed: 15215403]
48. Pollastri G, McLysaght A. Porter: a new, accurate server for protein secondary structure prediction. Bioinformatics 2005;21:1719–1720. [PubMed: 15585524]

49. Rost B, Sander C. Prediction of protein secondary structure at better than 70% accuracy. J Mol Biol 1993;232:584–599. [PubMed: 8345525]
50. Jones DT. Protein secondary structure prediction based on position-specific scoring matrices. J Mol Biol 1999;292:195–202. [PubMed: 10493868]
51. Vullo A, Bortolami O, Pollastri G, Tosatto SC. Spritz: a server for the prediction of intrinsically disordered regions in protein sequences using kernel machines. Nucleic Acids Res 2006;34:W164–W168. [PubMed: 16844983]
52. Dosztanyi Z, Csizmok V, Tompa P, Simon I. IUPred: web server for the prediction of intrinsically unstructured regions of proteins based on estimated energy content. Bioinformatics 2005;21:3433–3434. [PubMed: 15955779]
53. Obradovic Z, Peng K, Vucetic S, Radivojac P, Dunker AK. Exploiting heterogeneous sequence properties improves prediction of protein disorder. Proteins 2005;61:176–182. [PubMed: 16187360]
54. Uversky VN, Gillespie JR, Fink AL. Why are `natively unfolded' proteins unstructured under physiological conditions? Proteins 2000;15:415–427. [PubMed: 11025552]
55. Woody RW. Circular dichroism. Methods Enzymol 1995;246:34–71. [PubMed: 7538625]

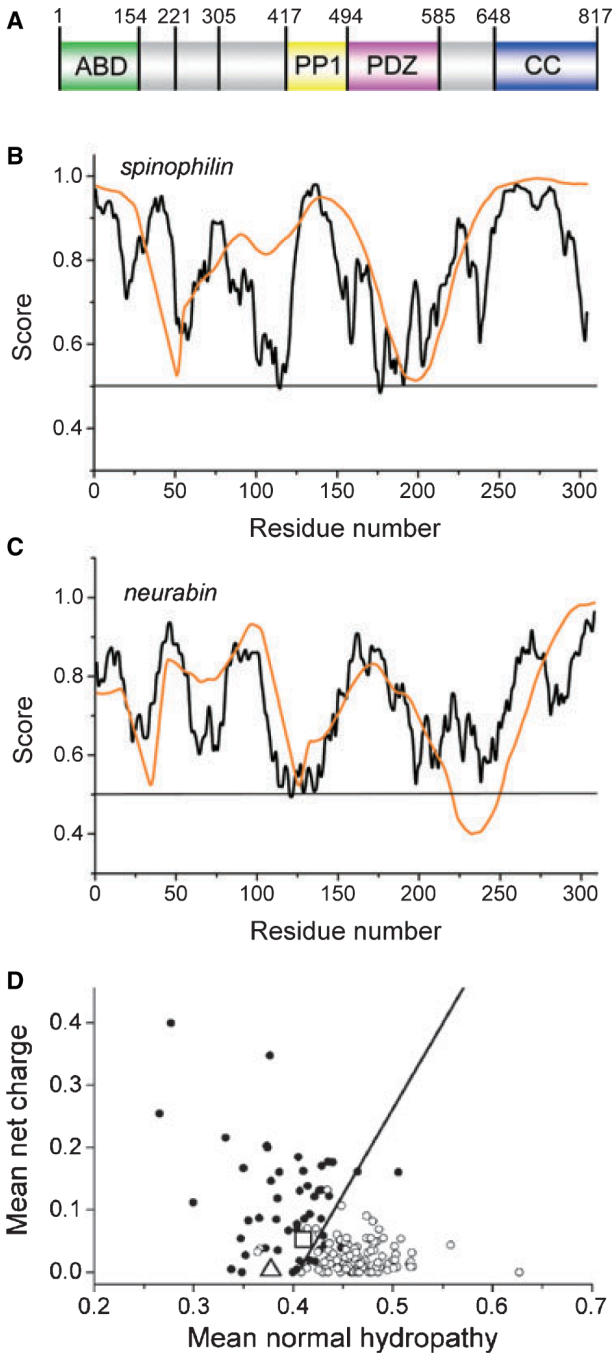

Fig. 1.

N-terminal F-actin binding domains of spinophilin and neurabin are predicted to be disordered. (A) Schematic representation of the *Rattus norvegicus* spinophilin sequence with the positions of the construct limits used in this study and domain borders indicated by numbers. The core actin binding domain, PP1 binding domain, PDZ domain and C-terminal coiled-coil region are indicated. (B, C) The sequences of human spinophilin (B) and neurabin (C) were analysed for disorder using the programs IUPRED (black lines) [52] and VSL2 (orange lines) [53]. Sequences scoring mostly above the value of 0.5 (indicated) are generally regarded as intrinsically disordered. (D) Charge hydropathy plots [54] for human spinophilin (square), neurabin (triangle) and reference sets of ordered (circles) and

disordered (dots) proteins. Both spinophilin and neurabin score above the discriminator line, indicating intrinsic disorder. The results of these analyses (B and D) for human and rat spinophilin were essentially identical.

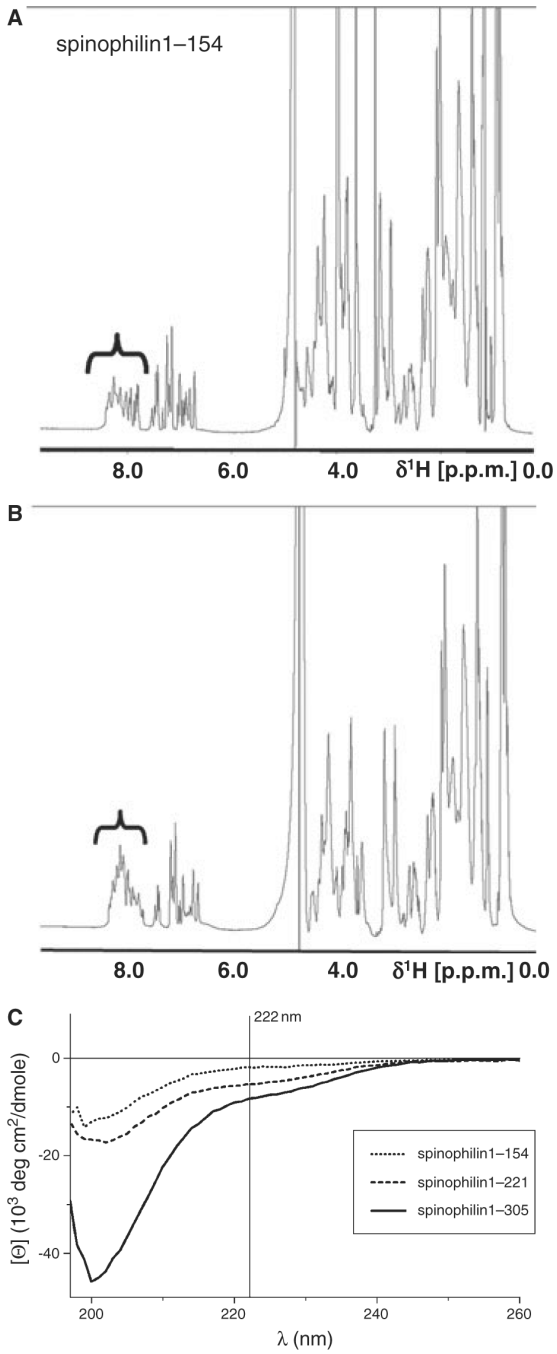

Fig. 2.

Recombinant proteins containing N-terminal fragments of rat spinophilin lack a regular secondary structure. (A, B) One-dimensional ^{1}H NMR spectra of residues 1–154 and 1–221 of spinophilin (spinophilin1–154 and spinophilin1–221), respectively. Parentheses indicate the dramatically reduced H^{N} chemical shift region because of the lack of a hydrogen bonding network in IUPs. (C) Far-UV CD spectra of spinophilin actin binding domain constructs. The molar ellipticity differences at 222 nm are highlighted by a black bar, clearly showing the differences in α-helical content in the three spinophilin actin binding domain constructs.

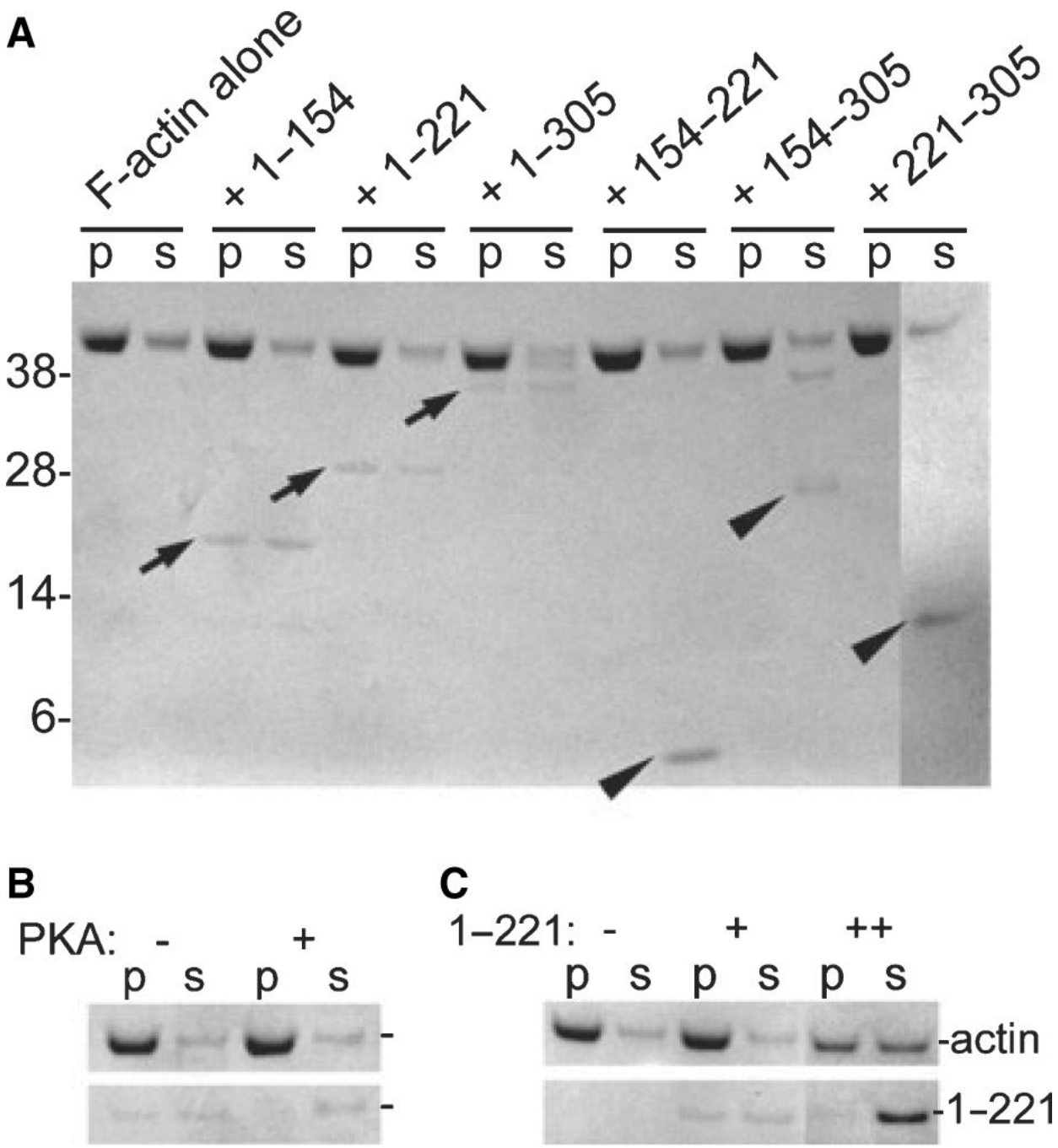

Fig. 3.

Recombinant proteins containing N-terminal fragments of rat spinophilin are active in F-actin binding. (A) Cosedimentation assays of 5 μM polymers of calf brain γ-actin and 2 μM spinophilin constructs. Residues 1–154, 1–221 and 1–305 of spinophilin are noticeably enriched in the pellet fractions on ultracentrifugation (arrows), indicative of F-actin binding, whereas residues 154–221, 154–305 and 221–305 of spinophilin do not cosediment with F-actin (arrowheads). (B) Cosedimentation assay of F-actin and residues 1–221 of spinophilin after incubation with PKA. The F-actin interacting capacity of residues 1–221 of spinophilin is reduced on PKA-mediated phosphorylation. (C) At equimolar amounts of residues 1–221

of spinophilin and F-actin, an apparent shift of actin from the pellet to the supernatant fraction can be observed.

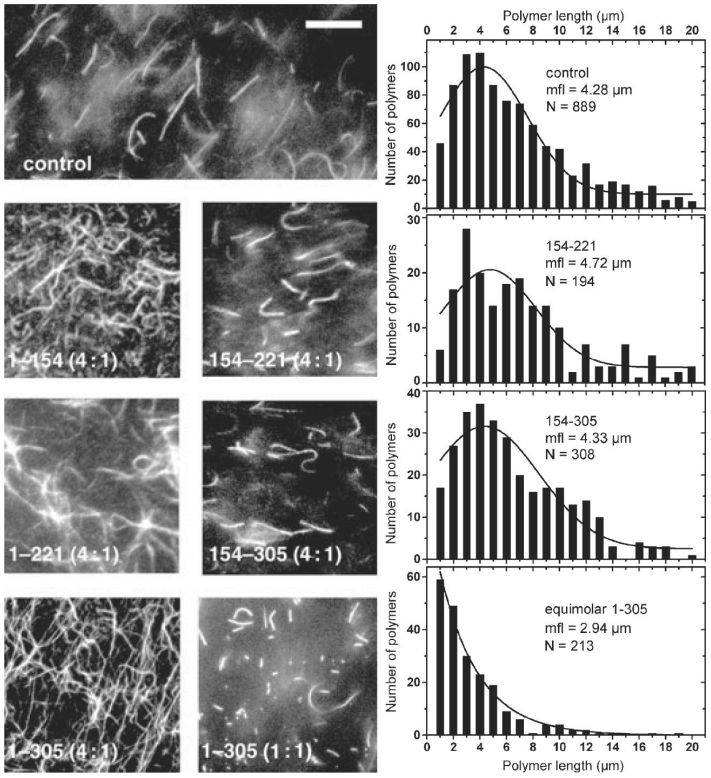

Fig. 4.

Spinophilin F-actin binding domain constructs can crosslink and cap actin polymers. Polymers of actin, marked with rhodamine–phalloidin, appeared elongated in the fluorescence microscope (top panel; space bar, 5 μm). The addition of low concentrations of residues 1–154, 1–221 and 1–305 of spinophilin induced crosslinking of actin polymers (4 : 1 actin to spinophilin molar ratio; left panels). By contrast, the addition of equimolar amounts of spinophilin constructs resulted in the disappearance of networks and fragmentation of actin polymers (shown for residues 1–305 of spinophilin, bottom right panel), suggesting a polymer capping activity of spinophilin. The histograms on the right show a quantitative analysis of the polymer length distributions of actin alone (control, top histogram) or in the presence of an equimolar amount of residues 1–305 of spinophilin (bottom histogram). Mean filament lengths (mfl) are given. The spinophilin constructs lacking F-actin binding capacity (residues 154–221 and 154–305 of spinophilin) had no impact on F-actin morphology, regardless of concentration.

Table 1

Summary of secondary structure predictions for N-terminal portions of human neurabin-1 (HsNEB1), human spinophilin (HsNEB2) and rat spinophilin (RnNEB2), calculated using six different prediction software programs.

	Random coil predictions (%)					
	APSSP2 [46]	**NORS [47]**	**PORTER [48]**	**PROF [49]**	**PSIPRED [50]**	**SPRITZ [51]**
HsNEB1 (1–308)	78.6	79.5	73.1	79.6	82.5	51.6
HsNEB2 (1–304)	79.3	89.8	74.0	89.8	81.1	60.9
RnNEB2 (1–305)	76.9	82.0	75.1	82.0	82.9	61.3